FFI RAPPORT

CAVITY EXPANSION THEORY APPLIED TO THE PENETRATION OF HIGH SPEED SPHERES INTO WEAK TARGETS

MARTINUSSEN Svein E, MOXNES John F

FFI/RAPPORT-2002/03291

FFIBM/778/130

Approved
Kjeller 4 June 2002

Bjarne Haugstad
Director of Research

CAVITY EXPANSION THEORY APPLIED TO THE PENETRATION OF HIGH SPEED SPHERES INTO WEAK TARGETS

MARTINUSSEN Svein E, MOXNES John F

FFI/RAPPORT-2002/03291

FORSVARETS FORSKNINGSINSTITUTT
Norwegian Defence Research Establishment
P O Box 25, NO-2027 Kjeller, Norway

FORSVARETS FORSKNINGSINSTITUTT (FFI)
Norwegian Defence Research Establishment

P O BOX 25
N0-2027 KJELLER, NORWAY

UNCLASSIFIED

SECURITY CLASSIFICATION OF THIS PAGE
(when data entered)

REPORT DOCUMENTATION PAGE

1) PUBL/REPORT NUMBER	2) SECURITY CLASSIFICATION	3) NUMBER OF PAGES
FFI/RAPPORT-2002/03291	UNCLASSIFIED	19
1a) PROJECT REFERENCE	**2a) DECLASSIFICATION/DOWNGRADING SCHEDULE**	
FFIBM/778/130	-	

4) TITLE

CAVITY EXPANSION THEORY APPLIED TO THE PENETRATION OF HIGH SPEED SPHERES INTO WEAK TARGETS

5) NAMES OF AUTHOR(S) IN FULL (surname first)

MARTINUSSEN Svein E, MOXNES John F

6) DISTRIBUTION STATEMENT

Approved for public release. Distribution unlimited. (Offentlig tilgjengelig)

7) INDEXING TERMS

IN ENGLISH:	IN NORWEGIAN:
a) Cavity Expansion	a) Hulrom ekspansjon
b) Penetration	b) Inntrenging
c) Soap	c) Såpe
d) Wound ballistics	d) Sår ballistikk
e)	e)

THESAURUS REFERENCE:

8) ABSTRACT

As a first attempt at identifying a tissue model for use in wound ballistic simulations a study of the deceleration of spherical steel projectiles in soap has been carried out. Experimental data were compared to numerical simulations using AUTODYN-2D, and to predictions given by cavity expansion theory.

We found that the AUTODYN-2D simulations show good agreement with experiment when a simple linear equation of state is used in conjunction with a Mieses strength model and a Pmin failure criterion . The predictions made using the cavity expansion theory do not agree well with experiments. A detailed investigation using the numerical model show that the cavity expansion theory agrees well only for the initial phase of the penetration. We believe that the dynamic part of the cavity expansion theory in general is wrong. Based on the theory for laminar flow and observations from AUTODYN-2D simulations, we propose improvements to the cavity expansion theory.

9) DATE	AUTHORIZED BY	POSITION
	This page only	
4 June 2002	Bjarne Haugstad	Director of Research

ISBN 82-464-0681-7

UNCLASSIFIED

SECURITY CLASSIFICATION OF THIS PAGE
(when data entered)

CONTENTS

CAVITY EXPANSION THEORY APPLIED TO THE PENETRATION OF HIGH SPEED SPHERES INTO WEAK TARGETS

1 INTRODUCTION

In this article we focus on the ability of the cavity expansion theory to facilitate wound ballistic computations. The Cavity Expansion Theory has in its simplicity constituted the foundation of penetration mechanics for more than 50 years. Forrestal [1] revived the theory by introducing the S function. Later it has been shown that the S function is not constant, and that it is not clear how predictive the theory is.

The cavity expansion theory assumes that the projectile is not deformed during the penetration process. At high impact velocities where hydrodynamic forces are large, the cavity expansion theory can usually not be used because the projectile deforms upon impact with the target. In these cases hydrodynamic theories for the flow of the projectile have to be used. In recent years, after the Gulf war, focus has shifted towards penetration of hardened targets using new penetrators. When considering for instance a Wolfram Carbide penetrator with a velocity of 1500m/s, even a concrete target may be considered a soft material, but hydrodynamic forces may still play a very important role.

The hydrodynamic forces are to a large extent dominant when projectiles penetrate tissue. In this article we study the penetration of steel spheres into soap which is a typical tissue simulator. Soap has a negligible mechanical strength at impact velocities of 1000m/s and upward. At the same time no turbulence occur for these cases and the flow pattern may be considered to be laminar. Use of steel spheres simplify the geometry, and allows analytic solutions to be found, at the same time as the numerical computations can be carried out in 2D.

To relate the cavity expansion theory to a penetration problem, on has to find a relation between the expansion velocity of the cavity, u, and the velocity of the penetrator, v. For spherical noses the relation $u=v\cdot\cos(\theta)$ is used, where θ is the angle between the penetration direction and a line from the centre of the spherical nose of the penetrator to the surface of the spherical nose. This relation is a weak link in the connection between the cavity expansion calculations and the penetration process. We will show that the theoretical pressure distribution on the penetrator nose does not agree, in the limit that the mechanical strength approaches zero, with the theory of incompressible laminar flow.

A series of experiments where steel spheres were shot at soap targets have been carried out [2]. Comparison with AUTODYN-2D simulations shows good agreement with recorded projectile exit velocities. The simulations and the experiments gave an overall drag coefficient of 0.36, while the cavity expansion theory gave 1.5. The pressure distribution on the front of the

spheres, as calculated in AUTODYN-2D, was considerably lower than the predictions of the cavity expansion theory, except for in the initial phase of the penetration.

If we demand that the penetration theory should correspond with the cavity expansion theory when the mechanical strength is dominant, and that it should correspond with the theory for laminar flow when the dynamic forces are dominant numerical simulations and experiments become reasonably close.

2 THE EXPERIMENTAL SET-UP

In figure 2.1 the experimental set-up used by Krogh and Omholt [2] is shown.

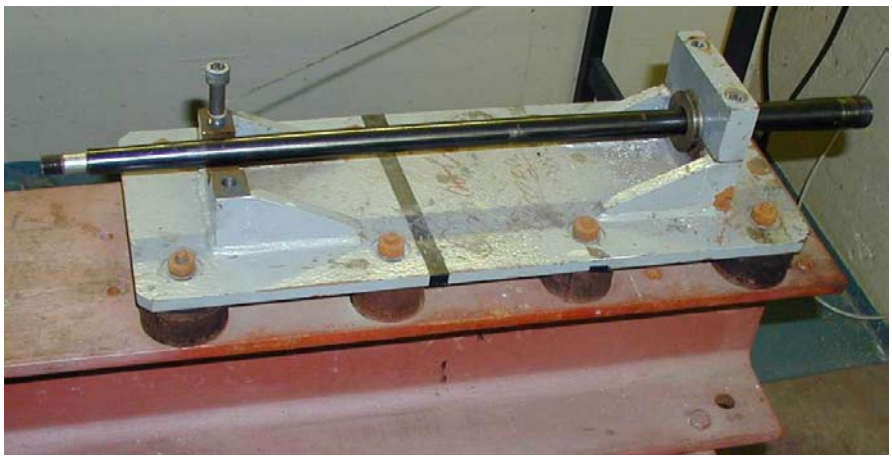

Figure 2.1 The experimental set-up (gun) used by Krogh and Omholt [2].

The velocity before and after penetration was measured by cross correlating signals from two coils in the front and in the back. Wound profiles where registered afterwards by cutting the soap block into two.

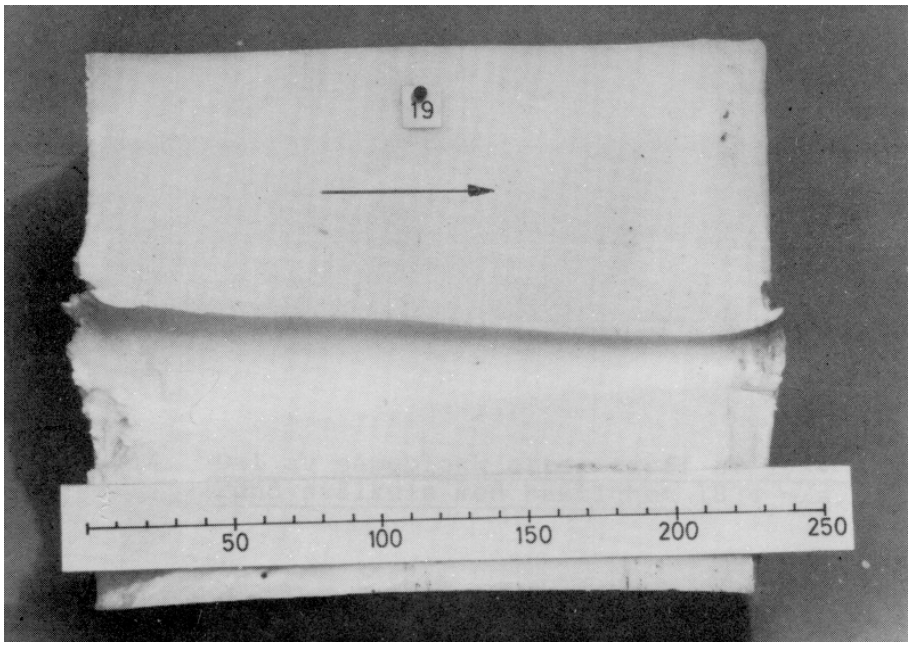

Figure 2.2 Soap block after being penetrated by a steel sphere at an initial velocity of 1258 m/s (the length scale is in mm). Length:23 cm,width:19.5 cm, quadratic in shape.

3 THEORETICAL BACKGROUND-THE DRAG COEFFICIENT

In this section we shall give a short description of the cavity expansion theory and the theory of laminar flow around a sphere.

The cavity expansion theory for a spherical projectile is based on a spherical cavity expanding in an infinite medium (figure 3.1). Computation of the radial stress in an elastic incompressible ideal plastic target gives:

$$\sigma_{rr} \overset{def}{=} -p + s_{rr} \tag{3.1}$$

The pressure is given by [3]:

$$p \overset{mod}{=} -\frac{3}{2}\rho_0 u^2 - \rho_0 r\dot{u} \tag{3.2}$$

where “mod” means a model assumption and “def” means a definition. The last part of the expression on the right hand side is negligible.

The mechanical part of the radial stress is according to the cavity theory [3] given by:

$$s_{rr} \overset{mod}{=} \frac{2}{3}Y\left(1+\log\left(\frac{2G}{Y}\right)\right) \quad \text{(alternative a)} \tag{3.3}$$

or:

$$s_{rr} \overset{mod}{=} \frac{7}{9} Y \log\left(\frac{2G}{Y}\right) \qquad \text{(alternative b)} \qquad (3.4)$$

where

u: radial velocity of the cavity wall
ρ_0: density of the target
Y: yield limit for the target
G: shear modulus for the target
r: radius of the spherical cavity

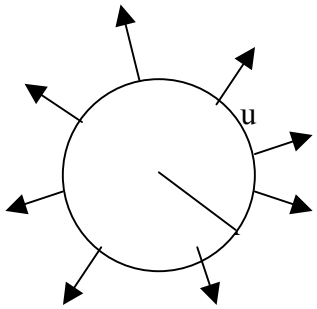

Figure 3.1 Cavity expansion in an infinite medium.

The cavity expansion velocity now has to be related to the penetration velocity. For a penetrator with a spherical nose the following assumption is made [3]:

$$u \overset{mod}{=} v \cos(\theta) \qquad (3.5)$$

where
θ: angle between the direction of penetration and a line from the centre of the sphere to the cavity surface (figure 3.2)
v: penetration velocity

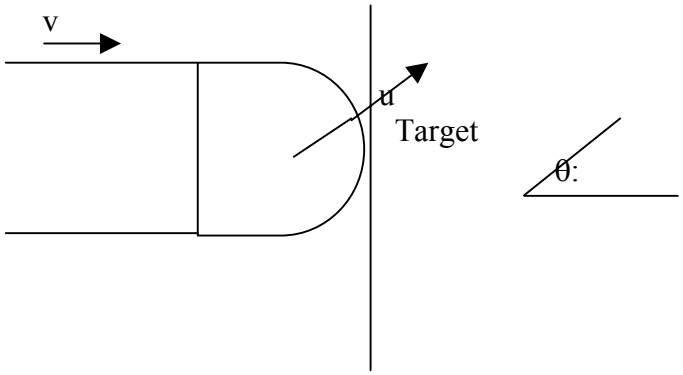

Figure 3.2 The relation between the penetration velocity and the cavity expansion velocity.

The force that decelerates the projectile can now be decomposed into two parts, F_{pc} from inertia (the hydrodynamic pressure) and F_{sc} from the stiffness of the material.

By integrating over the sphere surface we get:

$$F \overset{\text{def}}{=} \left(F_{pc} + F_{sc}\right) \tag{3.6}$$

$$F_{pc} = 2\pi R^2 \int_0^{\theta_c} \rho_0 v^2 \frac{3}{2}\cos^2(\theta)\cos(\theta)\sin(\theta)d\theta = \frac{3}{4} A \rho_0 v^2 \left(1 - \cos^4(\theta_c)\right) \tag{3.7}$$

where

R: radius of the spherical nose
A: πR^2, projected area of the spherical nose

θ_c in the initial phase depends on the degree of penetration, and is given by:

$$\theta_c = \theta_{cc} \overset{\text{def}}{=} Min\left(\frac{\pi}{2}, \arccos\left(1 - \frac{x}{R}\right)\right) \tag{3.8}$$

where

x: penetration depth

For a deviatoric part given by alternative a, we then have:

$$F_{sc} = 2\pi R^2 \int_0^{\theta_c} \frac{2}{3} Y \left(1 + \log\left(\frac{2G}{Y}\right)\right)\cos(\theta)\sin(\theta)d\theta = \frac{1}{3} AY \left(1 + \log\left(\frac{2G}{Y}\right)\left(1 - \cos(2\theta_c)\right)\right) \tag{3.9}$$

The drag coefficient that is due to the dynamic forces will then be given by:

$$\mathrm{Cd_{pc}}\left(\theta_c\right) \overset{\text{def}}{=} \frac{\mathrm{F_{pc}}}{\frac{1}{2}\rho_0 \mathrm{v}^2 \mathrm{A}} = \frac{3}{2}\left(1-\cos^4\left(\theta\right)\right) = 3\theta_c^2 - \frac{1}{4}\theta_c^4 + \mathrm{O}\left(\theta_c^6\right) \tag{3.10}$$

and the part that is due to the stiffness of the material is given by:

$$\mathrm{Cd_{sc}}\left(\theta_c\right) \overset{\text{def}}{=} 2\frac{\mathrm{F_{sc}}}{\mathrm{AY}\left(1+\log\left(\frac{2\mathrm{G}}{\mathrm{Y}}\right)\right)} = \frac{2}{3}\left(1-\cos\left(2\theta_c\right)\right) \tag{3.11}$$

After a penetration of length R the critical angle is according to (3.8) given by $\theta_c = \pi/2$. Then we have from (3.10) and (3.11) that

$$\mathrm{Cd_{pc}}\left(\pi/2\right) = 3/2 \tag{3.12}$$

$$\mathrm{Cd_{sc}}\left(\pi/2\right) = 4/3 \tag{3.13}$$

The pressure distribution on the surface of the sphere and $\mathrm{Cd_{pc}}$ may be compared to the predictions given by the theory of incompressible laminar flow. The pressure around a sphere that moves in an incompressible fluid at laminar flow conditions and no slip is given by [4]

$$p = -\frac{1}{8}\rho_0 \mathrm{v}^2\left(9\cos^2\left(\theta\right)-5\right) \tag{3.14}$$

This gives a force of:

$$\mathrm{F_p} = 2\pi \mathrm{R}^2 \int_0^{\theta_c} \frac{1}{8}\rho_0 \mathrm{v}^2\left(9\cos^2\theta - 5\right)\sin\theta\cos\theta \,\mathrm{d}\theta = \frac{1}{4}\mathrm{A}\rho_0 \mathrm{v}^2\left(1-\frac{9}{4}\cos^4\left(\theta_c\right)+\frac{5}{4}\cos\left(2\theta_c\right)\right) \tag{3.15}$$

The drag coefficient is then

$$\mathrm{Cd_p}\left(\theta_c\right) \overset{\text{def}}{=} \frac{\mathrm{F_{pc}}}{\frac{1}{2}\rho_0 \mathrm{v}^2 \mathrm{A}} = \frac{1}{2}\left(1-\frac{9}{4}\cos^4\left(\theta_c\right)+\frac{5}{4}\cos\left(2\theta_c\right)\right) = \theta_c^2 + \frac{7}{24}\theta_c^4 + \mathrm{O}\left(\theta_c^6\right) \tag{3.16}$$

From (3.19) and (3.16) it follow that

$$\lim_{\theta_c \to 0}\left(\frac{\mathrm{Cd_{pc}}}{\mathrm{Cd_p}}\right) = 3 \tag{3.17}$$

This shows that the theoretical pressure distribution on the penetrator nose does not agree with the theory of incompressible laminar flow for small angles.

From the material data in appendix A the following relation follows when the projectile leaves the soap after penetration:

$$\frac{F_{sc}}{F_{pc}} \sim \frac{8s_{rr}}{\rho_0 v^2} \sim 0.01 \tag{3.18}$$

This shows that the mechanical strength has negligible effect on the deceleration of a sphere. In figure 3.3 the drag coefficients from (3.10) (cavity) and (3.16) (lamflow) have been plotted as a function of θ_c up to $\theta_c=\pi/2$ when the penetration is larger than R. Also shown is an experimental curve (expflow) from fluid flow [5] at a Reynolds number of 3 10^5. The simulated curve is also shown (see next section).

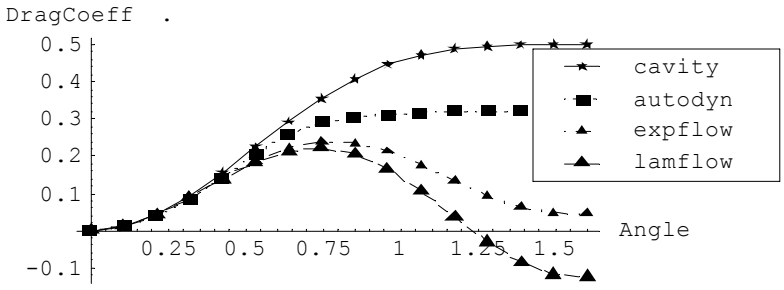

Figure 3.3 Different drag coefficients as a function of the angle. Cavity multiplied with 1/3.

4 AUTODYN SIMULATION AND EXPERIMENTAL RESULTS

In this section simulations in AUTODYN-2D will be compared to the experiments.

Figure 4.1 shows the Euler grid of the soap and the Lagrange grid of the spherical steel projectile.

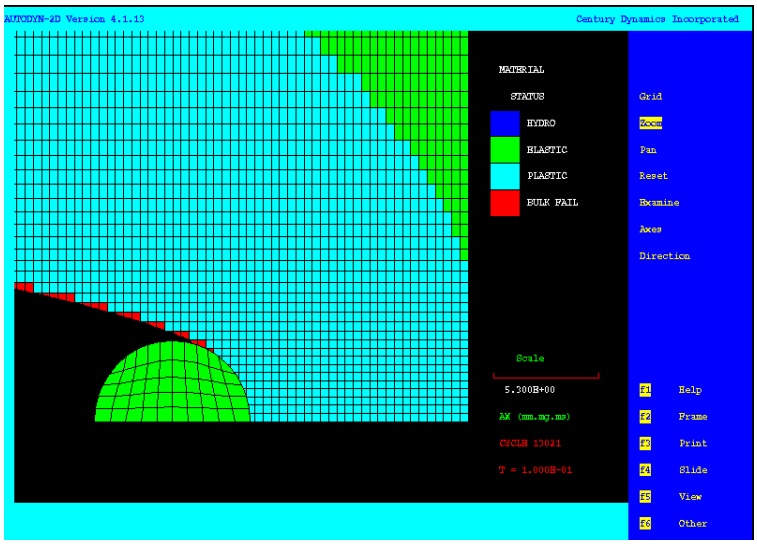

Figure 4.1 The grid of the target and projectile after 0.1 milli seconds.

In figure 4.2 the velocity of the projectile is shown as a function of penetration depth for shots with initial velocities of 1258, 1557 and 1834 m/s, respectively. Simulated exit velocities are in good agreement with experiment.

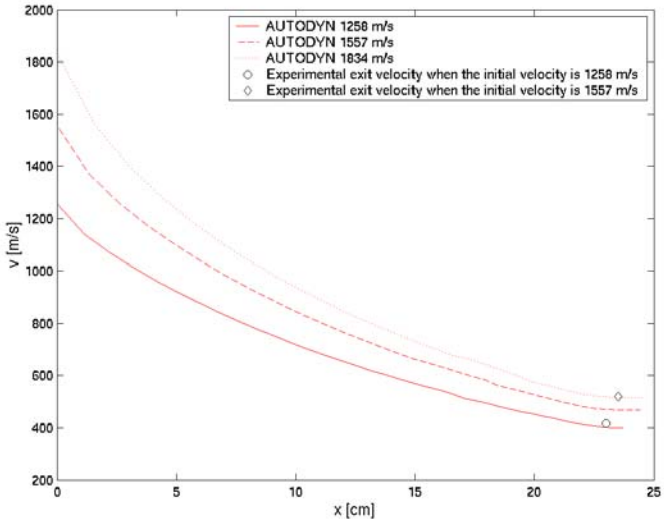

Figure 4.2 Simulated and experimental velocities as a function of the penetration depth.

In figure 4.3 the simulated normalised pressure ($p/\rho_0 v^2$) on the front of the projectile is shown as a function of the angle when the projectile has penetrated into the region (semi-infinite) where the slip angle should be $\pi/2$ according to the cavity expansion theory. The slip angle is 1.26 rad (72°). We observe from figure 3.3 that the contribution from the pressure to the drag coefficient is small for angles larger than 0.7. Figure (4.3) also shows that 1/3 of the pressure given from the cavity expansion theory is still too large compared with the simulations. We

can see that the laminar fluid pressure is much closer to the simulated pressure for angles less than 0.7. Also shown is the experimental result for fluid flow.

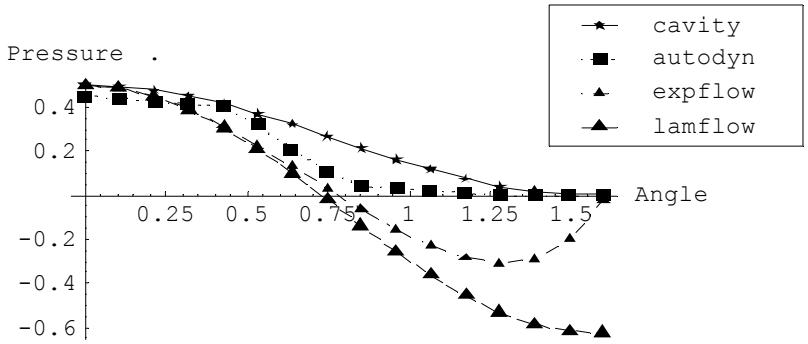

Figure 4.3 Normalised pressure profiles as a function of the angle at 0.1 ms. Cavity theory multiplied with 1/3.

In figure 4.4 the simulated drag coefficients is shown as a function of time. Also shown is the simulated drag coefficient in the semi-infinite region (0.36). Based on the observations made when doing the simulations on may describe the different parts of the penetration process:

1. The drag coefficient is dynamic, starting from zero and increases to 1.2 (close to the theory for cavity expansion) when the sphere has penetrated one radius. This is caused by the effectively increasing cross section of the projectile as it penetrates into the target.
2. The drag coefficient decreases as the sphere penetrates the target. It reaches a stable value of 0.36 when the sphere has penetrated approximately 10 radii into the target.
3. The drag coefficient remains stable at 0.36 for semi-infinite targets.
4. The drag coefficient is dynamic and oscillates around the stable value because of pressure waves being reflected back from the surface of finite targets.
5. When the sphere reaches the exit surface of the target the drag coefficient decreases again.

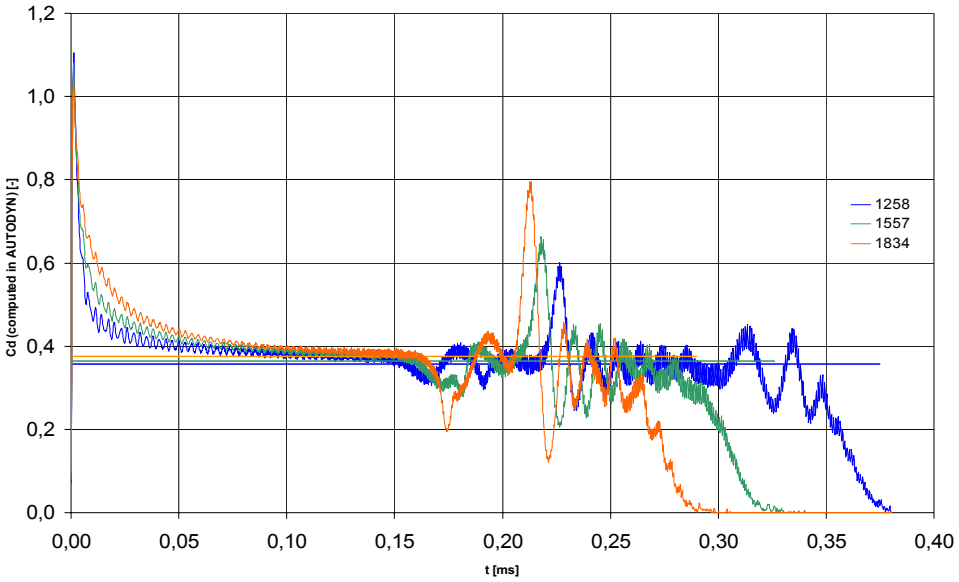

Figure 4.4 Drag coefficients for different initial velocities, time in milli seconds.

5 CONCLUSION/DISCUSSION

The AUTODYN-2D simulations have been found to give results that are in good agreement with the experiment, whereas the cavity expansion theory shows poor agreement with the experimental results except for in the initial phase of the penetration, before the sphere has penetrated one radius into the target. The pressure profile from the cavity expansion theory does not agree with the results from the AUTODYN-2D simulations in the phase where a stable drag coefficient is observed (semi-infinite region).

The cavity expansion theory can be improved if the theoretical pressure profile is divided by 3, and the slip angle is given by equation (3.8). This gives from figure (3.3) a reduction in the dynamic drag coefficient from 1.5 to 0.5 in the semi- infinite area of the penetration process.

Better results can be obtained if the slip angle is calculated more correctly. The cavity expansion theory predicts a slip angle of $\pi/2$ when the projectile has penetrated more than one radius since σ_{rr} is positive over the surface of the spherical nose. But by combining the solutions obtained by the theory of laminar flow and the cavity expansion theory, we obtain a solution that agree with both limiting conditions, v approaches zero or Y approaches zero, that is:

$$\sigma_{rr} = \frac{1}{8}\rho_0 v^2\left(9\cos^2(\theta_c) - 5\right) + s_{rr} \qquad (5.1)$$

where s_{rr} is given in equation (3.3) or (3.4). The slip angle can now be computed by letting $\sigma_{rr} = 0$, giving:

$$\theta_c = \theta_{cl} = Min\left(\frac{\pi}{2}, \arccos\left(\left(\frac{8s_{rr}}{\rho_0 v^2} + \frac{5}{9}\right)^{1/2}\right), \arccos\left(1 - \frac{x}{R}\right)\right) \tag{5.2}$$

As shown the mechanical strength of the soap has neglibible influence on the deceleration of the projectile for the cases reported here. We thereby have, when x is larger than R:

$$\theta_{cl} = 0.73 \quad (42^\circ) \tag{5.3}$$

The drag coefficient given from the laminar flow is then:

$$Cd_p(\theta_{cl}) = \frac{1}{2}\left(1 - \frac{9}{4}\cos^4(\theta_{cl}) + \frac{5}{4}\cos(2\theta_{cl})\right) = 0.22 \tag{5.4}$$

which is too low compared with 0.36 from the simulations. We observed in the simulations that the contribution to the pressure from angles larger than 0.7 is small. This result indicates that an applicable value for the slip angle is $\theta_c=\theta_{cl}$. Inserting this into 1/3 of the cavity result gives

$$Cd_{pc}(\theta_{cl}) = \frac{1}{2}\left(1 - \cos^4(\theta_{cl})\right) = 0.35 \tag{5.5}$$

This value for the drag coefficient is close to 0.36 observed in the simulations for the semi-infinite area of the penetration process. An average value over the hole penetration process is also approximately 0.36. It is expected that the same should apply for all penetrators with a spherical nose.

References

[1] Forrestal M. J., Penetration Into Dry Porous Rock, Int. J. Solids Structures Vol. 22, No 12, pp. 1485-1500, 1986.

[2] Krog T., Omholt L., FFI/Notat-81/4008.

[3] Bishop R. F., Hill R., Mott N. F., The Theory of Indentation and Hardness Tests, Proc. Phys. Soc. Vol.57, Part 3, No. 321, pp. 147-159, May 1945.

[4] Landau L. D., Lifshitz E. M., Fluid Mechanics, Pergamon Press 1987.

[5] White F. M., Viscous Flow, McGraw-Hill.

A APPENDIX

The following material parameters were used:

Steel Sphere: Radius: 3.97m.m. Mass::2.04 g, Yield stress: 1.8 10^9Pa
Soap:Length: 23cm,width:19.5cm, quadratic,density:1034 kg/m^3, Yield stress: 1. 0 10^6Pa
Shear modulus: 6.7 10^6Pa,Bulk modulus:2.65 10^9Pa,Pmin=-infinite.

DISTRIBUTION LIST

FFIBM **Dato:** 4 juni 2002

RAPPORTTYPE (KRYSS AV)	RAPPORT NR.	REFERANSE	RAPPORTENS DATO
X RAPP ☐ NOTAT ☐ RR	2002/03291	FFIBM/778/130	4 juni 2002
RAPPORTENS BESKYTTELSESGRAD		ANTALL EKS UTSTEDT	ANTALL SIDER
Unclassified		35	19
RAPPORTENS TITTEL		FORFATTER(E)	
CAVITY EXPANSION THEORY APPLIED TO THE PENETRATION OF HIGH SPEED SPHERES INTO WEAK TARGETS		MARTINUSSEN Svein E, MOXNES John F	
FORDELING GODKJENT AV FORSKNINGSSJEF		FORDELING GODKJENT AV AVDELINGSSJEF:	
Bjarne Haugstad		Jan Ivar Botnan	

EKSTERN FORDELING

ANTALL	EKS NR	TIL
1		Flo Land/AMK Postboks 25, 2831 Raufoss
3		Alf Øversveen Flo Land/AMK Postboks 25,2831 Raufoss

INTERN FORDELING

ANTALL	EKS NR	TIL
14		FFI-Bibl
1		Adm direktør/stabssjef
1		FFIE
1		FFISYS
1		FFIBM
1		FFIN
1		Bjarne Haugstad, FFIBM
1		Svein W Eriksen, FFIBM
1		John F Moxnes, FFIBM
1		Gunnar Ove Nevstad, FFIBM
5		Avd ktr, FFIBM
1		Svein E. Martinussen,FFIBM
1		Per K. Opstad,FFIBM
1		Trine Reistad,FFIBM
		FFI vev

FFI-K1 Retningslinjer for fordeling og forsendelse er gitt i Oraklet, Bind I, Bestemmelser om publikasjoner for Forsvarets forskningsinstitutt, pkt 2 og 5. Benytt ny side om nødvendig.